FEASIBILITY STUDY OF USING AN ELECTRON BEAM FOR PROFILE MEASUREMENTS IN THE SNS ACCUMULATOR RING.*

A.Aleksandrov, S.Assadi, S.Cousineau, V.Danilov, S.Henderson, M.Plum, Spallation Neutron Source, Oak Ridge National Laboratory, Oak Ridge, TN 37831, U.S.A.

P. Logatchov, A.Starostenko, Budker Institute of Nuclear Physics, Novosibirsk, Russia

Abstract

The electron beam probe method was suggested for measuring profiles in high power beams. In this method, deflection of a low energy electron beam by the collective field of the high intensity beam is measured. The charge density in the high intensity beam can be restored under certain conditions or estimated by various mathematical techniques. We studied the feasibility of using the electron beam probe for the SNS accumulator ring using computer simulations of the diagnostic setup. Realistic proton beam distributions were used in the simulations. Several profile calculation techniques were explored and the results are reported in this paper.

INTRODUCTION

The design goal for the SNS ring is to accumulate $1.4 \cdot 10^{14}$ protons per 1ms pulse at a 60Hz repetition rate. Achieving the design beam intensity with acceptable losses is a challenging task, which could be tackled more easily if reliable measurements of the beam profile in the ring are available. Very high beam power density precludes using wires or other interceptive devices for beam profile measurements at peak of stored current when information on the beam size is most important. Non-interceptive diagnostics using an electron beam probe has been successfully tested at several accelerators [1,2] but with a beam parameters which are very different from that of the SNS ring (see Table 1). The goal of the present work was to investigate the feasibility of using this technique for the SNS ring, study the range of required electron beam parameters, find the fundamental limitations and choose an appropriate profile reconstruction algorithm.

Table 1: SNS proton ring beam parameters.

Proton kinetic energy, E_k	1 GeV
Circumference, C	248 m
Longitudinal distribution length	160 m
Number of protons, N	$1.4 \cdot 10^{14}$
Vacuum chamber radius, R	0.1 m
Beam rms radius, r_b	0.01-0.02 m

*SNS is managed by UT-Battelle, LLC, under contract DE-AC05-00OR22725 for the U.S. Department of Energy. SNS is a partnership of six national laboratories: Argonne, Brookhaven, Jefferson, Lawrence Berkeley, Los Alamos and Oak Ridge.

RECONSTRUCTION ALGORITHMS

Tomography for 2-D Reconstruction

If we assume that the electron beam deflection is small, the velocity change is negligible, and we neglect the effect of the magnetic field, then the electron beam deflection angle due to the interaction with the proton beam electrical charge is given by:

$$(\quad , \quad) \quad \int_L \frac{e}{mv^2}(E_x \cos \qquad E_y \sin \quad)ds \,, \quad (1)$$

where e, m are the electron charge and mass, respectively, v is the velocity, E_x, E_y are the horizontal and vertical components of the proton bunch space charge electric field, is the angle of the electron beam trajectory with the horizontal axis of the vacuum chamber cross section, and is the impact parameter of the electron beam (see Fig. 1).

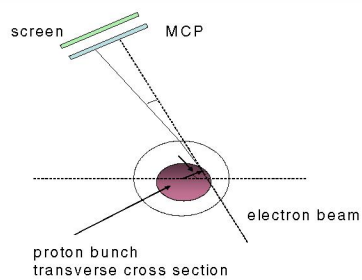

Figure 1: Setup layout for the electron tomography.

If we also assume that the electric field of the proton bunch is constant during an electron pass through the vacuum chamber then the net electron energy change is zero:

$$\int_L e(\quad E_x \sin \qquad E_y \cos \quad)ds \qquad 0 \cdot \quad (2)$$

By combining (1) and (2) we obtain,

$$\begin{aligned} &(\quad , \quad) \cos \qquad \int_L \frac{e}{mv^2} E_x ds \,, \\ &(\quad , \quad) \sin \qquad \int_L \frac{e}{mv^2} E_y ds \,. \end{aligned} \quad (3)$$

We have two similar integral equations for the horizontal and vertical components of the electric fields. These exact integral equations are solved by Radon in 1917 and are in use for conventional tomography (see e.g. [3]). The integral equation for tomography reads:

$$\hat{f}(\ ,\ ) \quad \int_L f(x,y)ds, \tag{4}$$

where $0< <2$ and $0< <$ are the integration parameters, and the integration path L is determined by the following relation: $,L \quad \{\{x,y\}: x\cos \quad y\sin \quad \}$ with being the angle of the integration line with the horizontal axis. This is same form of the equation we have in (3). The inversion formula is the following:

$$f(x,y) \quad \frac{1}{4^{\ 2}}\oint\int \frac{\hat{f}(\ ,\ )}{x\cos \quad y\sin }d\ d\ . \tag{5}$$

It should be noted that a variety of effective methods for numeric evaluation of (5) has been developed for numerous applications of tomography [3].

Finally, the proton beam density distribution (x,y) can be calculated using Maxwell equation for the electric field:

$$_0\left(\frac{E_{\ x}}{x} \quad \frac{E_{\ y}}{y}\right) . \tag{6}$$

In order to restore the 2-dimensional charge density distribution using the tomography formalism described above, a set of measurements with varying angle between the probe beam and the measured beam has to be performed, which requires rotating the diagnostic device around the measured beam or using multiple stationary devices at fixed angles. Technically, a full implementation can be difficult or cost prohibitive, but meaningful and useful information can be extracted even from measurement at single fixed angle, as shown below.

One-dimensional Profile Reconstruction

Lets assume that the electron beam deflection is measured on trajectories with different at 0. Then (1) becomes:

$$_0(x) \quad (0,\ ) \quad \int_L \frac{e}{mv^2}E_x dy \ , \tag{7}$$

after differentiating:

$$\frac{d\ _0(x)}{dx} \quad \int_L \frac{e}{mv^2}\frac{E_x}{x}dy \tag{8}$$

and using (2) and (7):

$$\frac{d\ _0(x)}{dx} \quad \int_L \frac{e}{mv^2}\left(— \quad \frac{E_y}{y}\right)dy \quad \frac{e}{mv^2}\left(\int_L —dy \quad —y\int_L E_y dy\right).$$

From (2): $\int_L E_y dy \quad 0$ at $\quad 0$,and therefore finally

$$\frac{d\ _0(x)}{dx} \quad \int_L \frac{e}{mv^2}\frac{(x,y)}{\ _0}dy. \tag{9}$$

We see from (9) that derivative of the electron beam deflection angle with respect to the impact parameter gives the projection of the charge distribution on the x axis or, in other words, the beam profile, as it would be measured by an usual wire scanner. A successful implementation of this approach is described in [2].

Validity of the Approach

Several important assumptions were made in deriving the reconstruction formalism above. The validity of those assumptions depends on the physical implementation of the device and can't always be completely satisfied. For example, we assumed that the electron velocity doesn't change during its passage, which means the electron energy is much higher than the proton beam electric potential. In the SNS ring the beam potential can reach 10-20 kV depending on the location. This means that the electron probe energy should be at least in the 100 kV range, where we start to violate the assumption of non-relativistic motion. There are also unavoidable errors introduced by the final size of the electron beam at the interaction region and on the detector, etc. The effect of each of such deviations from the idealized model on the deflection angle can be analyzed relatively easily but it's hard to trace what the combined effect on the accuracy of the reconstruction. Therefore, we chose a computer simulation approach, when these effects can be modeled, for the feasibility study.

FEASIBILITY STUDY

Computer Simulations

We used the ORBIT simulation code [4] to trace electron trajectories in the space charge field of the accumulated proton bunch. It allows calculating e/m fields for arbitrary distributions in open space or in a circular or rectangular conducting chamber.

We used standard linear transform functions from the MATLAB image processing toolbox [5] to calculate inverse Radon transforms of the data from ORBIT.

We have specialized code to simulate electron beam in the electron gun and transport line before entering the ring vacuum chamber. We have not used that option yet and limited our study to single particle tracking.

We compared the original and the restored charge distributions for several different distributions: uniform axially symmetric in an open and in a circular conducting chamber, elliptical uniform, parabolic axially symmetric, and the realistic SNS beam in a circular conducting chamber. Simulations were done for different electron beam energy and proton beam charge.

Results

The dependence of the deflection angle on the impact parameter for different electron beam energies and proton beam charges is shown in Fig. 2. The deflection angle exceeds 0.1 radians at nominal beam current for electron beam energies below 75 kV. The deviation from the idealized model (separation of solid blue and dashed red lines in Fig.2) is clear at energies below 100kV.

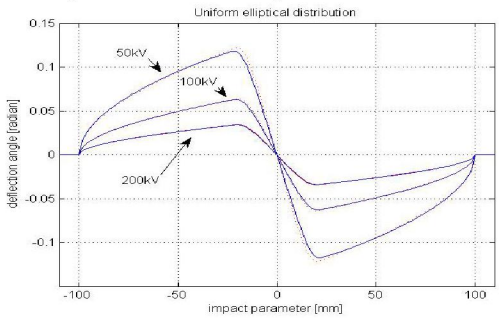

Figure 2: Dependence of the deflection angle on impact parameter for different electron beam energies and proton beam charges. Solid line (blue) – $1.5{\cdot}10^{14}$ protons/beam; dashed line (red) $-0.5{\cdot}10^{14}$ protons/beam, multiplied by 3.

The proton beam density distribution reconstructed using the inverse Radon transform is shown in Fig. 3 for the uniform elliptical distribution (coasting beam) and the expected SNS distribution (bunched beam). The final width of the transition from zero to flat top, and some non-uniformity in the flat top, is observed in the case of the elliptical distribution.

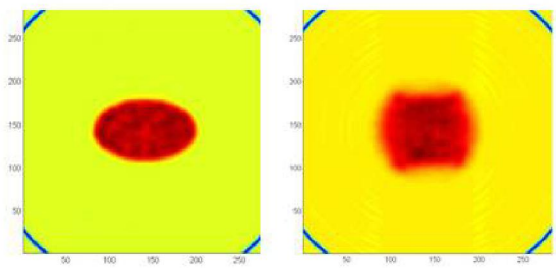

Figure 3: Reconstructed charge densities for uniform elliptical (left) and "real" SNS (right) distributions.

The cross section of the elliptical distribution in Fig. 4 shows that the flat top irregularity doesn't depend much on the electron beam energy or the proton beam charge. Most likely it is artifact of the discrete inverse Radon transform and its elimination would require refinement of the digital filter parameters and interpolation scheme. The transition width, on the other hand, depends on the electron beam energy and the proton beam charge and is ~5mm, in the best case. Note that this example represents an extreme case of sharp transition but the resolution for smoother distributions can be significantly better.

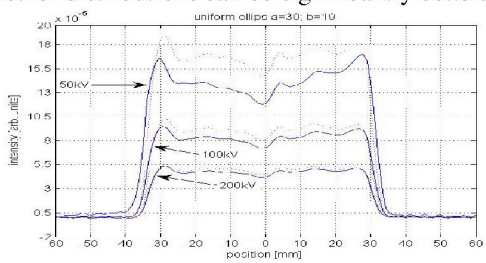

Figure 4: Cross section of the reconstructed elliptical distribution for different electron beam energies and proton beam charges. Solid line (blue) $-1.5{\cdot}10^{14}$ protons/beam; dashed line (red) $-0.5{\cdot}10^{14}$ protons/beam, multiplied by 3.

A comparison of the beam profile reconstructed from the single scan using (9) with ideal profile of the elliptical distribution is shown in Fig. 5. There is good agreement but again boundary lengthening of ~5 mm is observed, which is more pronounced for the lower energy 50 keV beam. More importantly, there is a significant effect from the vacuum chamber presence (sharp spikes at the edges and base line shift)

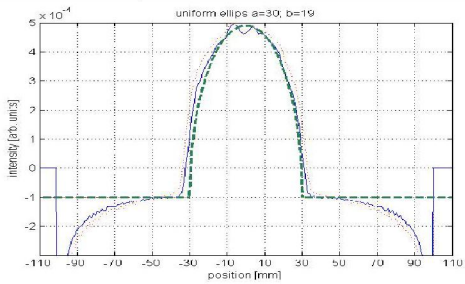

Figure 5: The reconstructed beam profile for the uniform elliptical distribution. Solid line (blue) – 200 kV; dashed line (red) – 50 kV, Dashed green line–analytical.

CONCLUSION AND FUTURE PLANS

As a result of our work we conclude that it's feasible to use electron beam probe diagnostics for profile measurements in the SNS ring. We are sure that attainable resolution will allow useful beam size measurements comparable with alternative techniques. We leave accurate estimating of the resolution to further studies, which will include realistic parameters of the electron gun and the detector. There are no expectations for measuring low level tails or halo.

REFERENCES

[1] Starostenko, et al., in Proceedings of the PAC99
[2] Roy, et al., Rev.Sci.Instrum. 76, 023301 (2005)
[3] A.G. Ramm et al, "The Radon Transform and Local Tomography", CRC Press, Inc., (1996)
[4] J.Holmes, et al., ICFA Beam Dynamics Newsletter No. 30,(2003). P.100
[5] http://www.mathworks.com/